

Wormlike Chain Theory and Bending of Short DNA

Alexey K. Mazur*

CNRS UPR9080, Institut de Biologie Physico-Chimique, 13, rue Pierre et Marie Curie, Paris, 75005, France

(Received 27 February 2007; published 24 May 2007)

The probability distributions for bending angles in double helical DNA obtained in all-atom molecular dynamics simulations are compared with theoretical predictions. The computed distributions remarkably agree with the wormlike chain theory and qualitatively differ from predictions of the subelastical chain model. The computed data exhibit only small anomalies in the apparent flexibility of short DNA and cannot account for the recently reported AFM data. It is possible that the current atomistic DNA models miss some essential mechanisms of DNA bending on intermediate length scales. Analysis of bent DNA structures reveal, however, that the bending motion is structurally heterogeneous and directionally anisotropic on the length scales where the experimental anomalies were detected. These effects are essential for interpretation of the experimental data and they also can be responsible for the apparent discrepancy.

DOI: [10.1103/PhysRevLett.98.218102](https://doi.org/10.1103/PhysRevLett.98.218102)

PACS numbers: 87.14.Gg, 87.15.Aa, 87.15.He, 87.15.La

The bending dynamics of double helical DNA on length scales of several helical turns plays a key role in many cellular processes [1]. This length scale is also crucial for the coupling between the atomistic DNA structure and its macroscopic mechanics. Long DNA double helices are well described by the classical wormlike chain (WLC) model with a persistence length of $A \approx 50$ nm [2], but for chain lengths shorter than A the validity of the WLC theory is uncertain [3,4]. Anomalously high flexibility was sometimes observed for double helices as short as 40 nm that exhibited experimental cyclization rates several orders of magnitude beyond the WLC predictions [3]. Until now, a few theories proposed to account for these anomalies did not converge to a consensus interpretation [5–7]. Very recently, AFM imaging experiments with direct counting of DNA bends in planar deposits revealed strong deviations of bend angle distributions from the WLC theory for chain length 5–20 nm [8]. In addition, these data disagreed with all alternative theories except the so-called subelastical chain model (SEC) [7]. However, statistical analysis of molecular dynamics (MD) trajectories indicates that atomistic DNA models agree with the WLC theory already for double helices of 1–2 helical turns [9]. This apparent controversy suggests either that earlier analysis of MD data was not complete or that MD simulations miss some essential molecular mechanisms of DNA bending.

In this Letter we present the first accurate comparison of analytical theories with DNA bend angle distributions observed in realistic MD simulations and try to get insight in the possible origin of anomalies in the apparent DNA flexibility on intermediate length scales. The MD data used here were obtained in long MD simulations of double helical DNA fragments of 25 base pairs (bp) with the AT-alternating sequence. For our present purposes this model system can be considered as homopolymer. The same data were already used for evaluation of elastic parameters of atomistic DNA models [9] and we refer the reader to this earlier paper for simulation details. Three MD trajectories

denoted AT25a-c, respectively, differed by hydration conditions as well as the number of degrees of freedom in the DNA duplexes. In AT25a (16 ns) DNA was modeled with all degrees of freedom in a rectangular water box with a neutralizing number of sodium ions. In AT25b (28 ns) the hydration conditions were the same as in AT25a, but the duplex was modeled with fixed geometry of chemical groups, rigid bases and only partially flexible backbone. In AT25c (120 ns) the minimal *B*-DNA model was used, with semi-implicit treatment of solvent as described earlier [10]. The analysis below uses the data from trajectory AT25a by default, but the results and conclusions were qualitatively similar for all three trajectories. For better sampling, statistical analysis included all internal fragments of a given length in the 25-mer DNA.

The WLC theory approximates the bending probability by the Gaussian distribution [2,11]

$$w_0 \sim \exp\left(-\frac{A}{2L}\theta^2\right), \quad (1)$$

where θ is the bend angle, L is the length of the DNA fragment, and A is the persistence length. Equation (1) is valid for sufficiently small L and θ , which is very well fulfilled for practical MD simulations. Assuming spherical isotropy of vector orientations randomly sampled in 3D space the differential of the probability distribution for small bend angles can be written as

$$\begin{aligned} dP &\sim \exp\left(-\frac{A}{2L}\theta^2\right) \sin\theta d\theta \\ &\approx \exp\left[-\frac{A}{L}(1-\cos\theta)\right] d(1-\cos\theta). \end{aligned} \quad (2)$$

Equation (2) indicates that the plots of the WLC probability density would give descending straight lines in coordinates: $(\ln P)$ vs $(1-\cos\theta)$, with variation of slopes governed by the DNA persistence length.

The SEC theory [7] does not predict the shapes of angle distributions for all chain lengths. It postulates that there exists an intermediate DNA length l_0 for which the bending probability is exponential

$$w_1 \sim \exp(-\alpha\theta). \quad (3)$$

Parameters l_0 and α have been estimated as 2.5 nm and 6.8, respectively [8]. For $L < l_0$, the SEC behavior is undefined, whereas for $L > l_0$ all its statistical properties converge to the WLC model due to the central limiting theorem. By applying the considerations of Eqs. (1) and (2) we see that the SEC probability density would give a descending straight line for $L = l_0$ in coordinates: $-(\ln P)^2$ vs $(1 - \cos\theta)$.

Figure 1 compares the shapes of DNA bend angle distributions obtained in the most detailed representation (AT25a) with the WLC and SEC theories. The agreement with the WLC theory is remarkable. The MD distributions in Fig. 1(a) are nearly linear and for $N \geq 6$ they agree very well with the WLC theoretical predictions shown by the dashed red straight lines. All these theoretical traces correspond to one and the same persistence length equal to the earlier reported value obtained from these MD data by different methods [9]. In contrast, Fig. 1(b) shows that these MD distributions systematically deviate from the SEC theoretical predictions. Qualitatively, the deviations in Fig. 1(b) are similar for all chain length suggesting that the SEC critical length l_0 can only be smaller. At the same time, Fig. 1(a) reveals for DNA fragments of 4–10 bp noticeable upward deviations of the tails of the distributions with respect to the linear regression lines obtained for small angles only, which qualitatively agrees with the SEC assumption. Similar patterns were obtained for trajectories AT25b and c. The deviations from the WLC theory revealed in Fig. 1(a) are smaller than necessary for the correspondence with the SEC model, nevertheless, they are reproducible and require explanation.

The nonlinearities seen in Fig. 1(a) can be rationalized if the population of DNA fragments of a given length is heterogeneous as regards elastic properties. For instance, if 50% of 10 mers are rigid while the rest 50% are more flexible the probability density for small angles would decrease more rapidly than expected for the average persistence length [see solid straight lines in Fig. 1(a)] In contrast, large bends can still occur due to the second group and the probability density plots in Fig. 1(a) would deviate upward. For homopolymer DNA such heterogeneity can originate from the intrinsic frustration in the *B*-DNA structure as suggested by the compressed backbone hypothesis (CBH) [12–14], and Fig. 2 reveals its possible mechanism. It is seen that the minor groove of this DNA fragment exhibits quasiregular modulations with a distinguished period of about 8 bp. This behavior originates from the compressed state of the backbone in the *B*-DNA structure as described elsewhere [12,13]. The DNA bending and

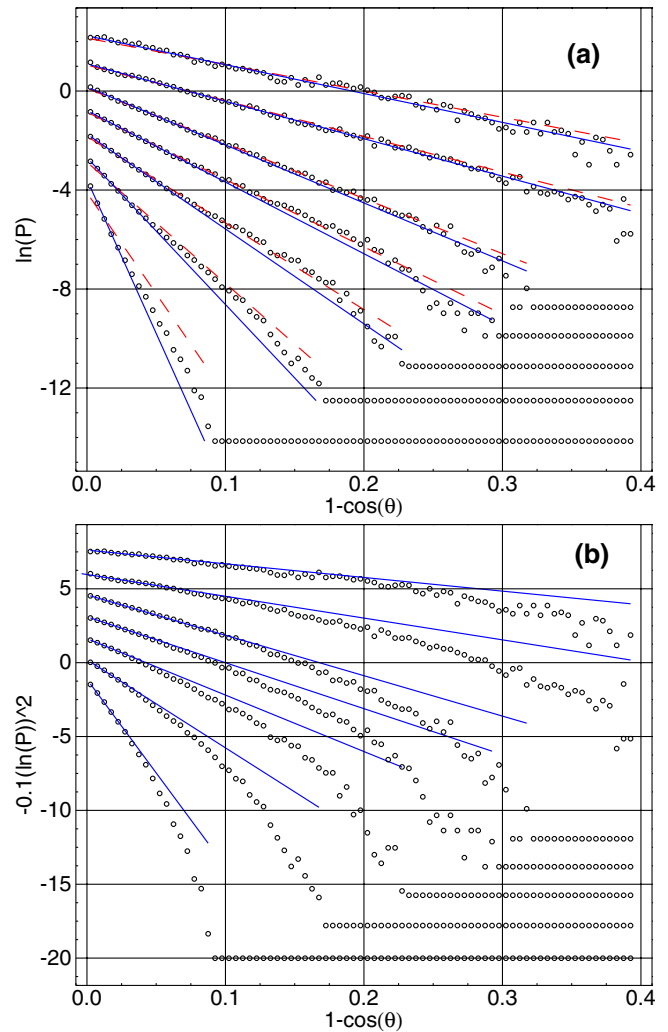


FIG. 1 (color online). Probability distributions of bend angles in DNA fragments of $N = 4, 6, 8, 10, 12, 18,$ and 24 bp. Data counts were accumulated in 80 windows evenly spaced on $0.6 < \cos\theta < 1$. (a) The y coordinate is chosen to linearize the WLC angle distributions. Red dashed lines correspond to WLC distributions with $A = 80$ nm (the value earlier obtained from the same data by other methods [9]). Blue solid lines represent linear regression analysis of the initial decrease down to e^{-2} including at least 5 points. All plots are consecutively shifted by one for clarity. (b) The y-coordinate is chosen to linearize the SEC angle distribution. Blue solid lines represent linear regression analysis of the initial decrease down to e^{-3} including at least 5 points. All plots are consecutively shifted by 1.5.

groove dynamics are not directly linked, but uneven minor groove profile can facilitate or hamper bending in certain directions. Now consider the ensemble of DNA fragments of 10 bp, for instance. This length is sufficient to accommodate one widening of the minor groove flanked by two narrowings, or one narrowing flanked by two widenings. If the bendability in these two subensembles strongly differ one would expect to observe the kind of deviation seen in Fig. 1(a) for 10-mers. More precisely, Fig. 2 indicates that a

DNA fragment of length L has at least $n = 8$ equally probable, but qualitatively different configurations of the minor groove profile. Assuming that in each of these subpopulations bending is approximately Gaussian, the overall bending probability can be expanded as

$$w(L) \sim \sum_{i=1}^n \exp[-\alpha_i(L)(\theta - \theta_i)^2]. \quad (4)$$

The possibility of static bends, that is $\theta_i \neq 0$, should not be excluded here. When L is comparable with the period of groove modulations the values of α_i and θ_i can vary giving a non-Gaussian overall distribution of bend angles. For longer chains the heterogeneity of α_i and θ_i should gradually disappear.

To verify the foregoing interpretation we compared the minor groove profiles in weakly and strongly bent conformers. The results are shown in Fig. 3(a). On average, the minor groove of 10-mer fragments is relatively even, which might be expected from the dynamics shown in Fig. 2(b). In contrast, strongly bent conformers tend to have a widening in the middle flanked by narrowings. This formally proves that parameters α_i and θ_i in Eq. (4) vary, which explains deviations from linearity seen in Fig. 1(a). In addition, Fig. 3(b) shows that strong bends in 10-mers

preferably occur towards the major groove in the middle, that is away from the central widening and towards the flanking narrowings of the minor groove in Fig. 3(a). Given the pattern displayed in Figs. 2(b) and 3(a), this effect does not seem surprising since it agrees with the earlier known general trends characteristic of curved DNA [15]. However, it points to another possible source of anomalies in the experimental distribution of bend angles in planar AFM images [8]. The 10-mer fragments of a long double helix deposited on a plane face it by all their sides with equal probability. If the pattern revealed in Fig. 3 remains valid for planar depositions, 10-mer fragments with the center of the major groove turned towards or away from the plane should on average look stiffer than those where the preferred bend direction revealed in Fig. 3(b) is parallel to the plane. Indeed, bends in directions perpendicular to the plane can be completely blocked or hindered, but anyway they are not detectable in AFM images. This effect can be expected to persist for DNA length of 10–20 bp and it can introduce an additional hidden heterogeneity in the ensembles of planar DNA segments of a given length.

The character of bending revealed in Figs. 2 and 3 indicates also that the specific atomistic structure of bent DNA may interfere with the very process of DNA deposition on a plane. Indeed, the preferred period of 8 bp for the minor groove modulations revealed in Fig. 2(a) together with the pattern shown in Fig. 3 indicates that strong bends

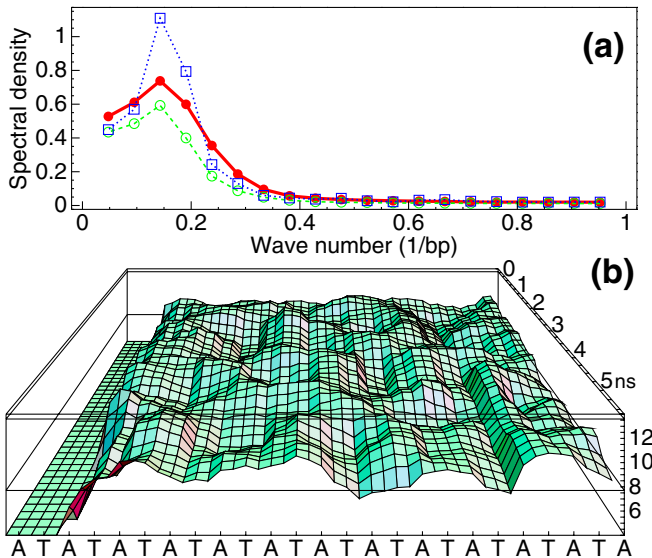


FIG. 2 (color online). (a) The average Fourier spectra of the profiles of the minor groove for three trajectories of the 25-mer AT-alternating fragment. AT25a—solid red line and filled circles; AT25b—dashed green line and open circles; AT25c—dotted blue line and open squares. The width of the minor groove was measured as described elsewhere [20] for all saved states and used for spectral analysis. Thus obtained spectral densities were averaged over the entire trajectories. (b) An example of time evolution of the minor groove profile. The surface plot is formed by 40 evenly spaced profiles taken on a sample 6 ns interval from trajectory AT25a. Every profile was averaged over 500 ps.

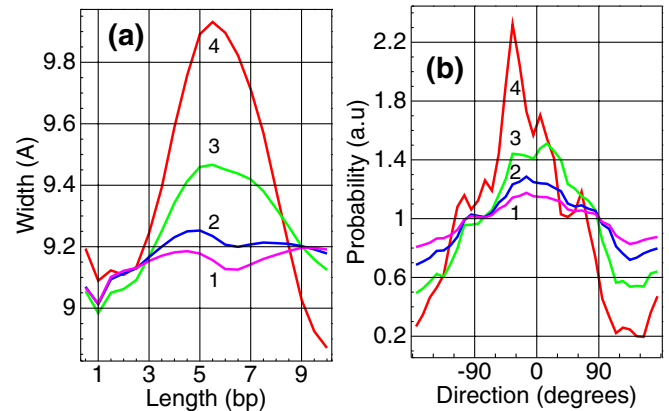


FIG. 3 (color online). (a) The average minor groove profiles evaluated in 10 bp DNA stretches sorted by the amplitude of bending. 1 (magenta)—overall ensemble average; 2 (blue)—fragments bent by more than 10° ; 3 (green)—fragments bent by more than 20° ; 4 (red)—fragments bent by more than 30° . The traces were smoothed with a sliding window of 2 bp to remove the sequence effect. (b) Radial distributions of bending direction in subensembles of 10 bp fragments used in plate (a). The bending direction is defined by the polar angle of the projection of the opposite ends upon the middle plane as described elsewhere [12]. The zero angle is chosen to correspond to a planar bend towards the major groove in the middle of the 10-mer. Colors and numbering are same as in plate (a). All plots are normalized by the small radial distribution corresponding to bend angles below 10° .

in the neighboring stretches of long DNA tend to occur in nearly perpendicular directions. This short-range correlation is incompatible with planar geometry and it should be somehow cancelled during deposition and equilibration of 3D DNA on a plane, which can produce unpredictable effects upon the distribution of bend angles.

The results presented in this Letter demonstrate that the probability distributions for bending angles in short stretches of double helical DNA obtained with the most accurate currently used atomistic models remarkably agree with the WLC theory already for lengths of about one helical turn. Recent molecular dynamics (MD) simulations of circular DNA indicated that strong bends in double helices may occur due to localized kinking, rather than smooth curvature corresponding to the WLC model [16,17]. In both cases, however, the kinks could be due to external factors like excessive bending strain [16] or protein-DNA contacts [17]. In the present studies, the contribution of kinks was not significant even in the strongest bends. It is hardly possible that longer MD simulations would change this conclusion for the range of bend angles sampled here. The ensemble of earlier MD studies of free DNA [18] evidences that breaking of base pair stacks like in Ref. [16] is never observed, probably because of high energy barriers. Therefore, to affect the populations of bend angles in the range sampled here, such states have to be very long-living, and the question arises why such states were not be detected in earlier NMR and x-ray studies [19]. At the same time, our results do not rule out the possibility of kinked states for very large angles not sampled here.

Our data do not agree with the recent report on anomalously high flexibility of DNA fragments of 5–17.5 nm detected by AFM experiments, as well as the SEC theory that explained these experimental data. It is possible that the present day atomistic DNA models do not reproduce some essential aspects of DNA bending on intermediate length scales. Analysis of bent DNA structures reveals, however, that, in spite of the good agreement with the WLC theory, the bending motion is structurally heterogeneous and directionally anisotropic on the intermediate length scales where the experimental anomalies were de-

tected. These effects are essential for interpretation of the experimental data and they also can be responsible for the apparent discrepancy.

*Electronic address: alexey@ibpc.fr

- [1] J. Widom, *Q. Rev. Biophys.* **34**, 269 (2001).
- [2] C. R. Cantor and P. R. Schimmel, *Biophysical Chemistry, Part III: The Behavior of Biological Macromolecules* (W. H. Freeman, San Francisco, 1980).
- [3] T. E. Cloutier and J. Widom, *Proc. Natl. Acad. Sci. U.S.A.* **102**, 3645 (2005).
- [4] Q. Du, C. Smith, N. Shiffeldrim, M. Vologodskaja, and A. Vologodskii, *Proc. Natl. Acad. Sci. U.S.A.* **102**, 5397 (2005).
- [5] J. Yan and J. F. Marko, *Phys. Rev. Lett.* **93**, 108108 (2004).
- [6] P. A. Wiggins, R. Phillips, and P. C. Nelson, *Phys. Rev. E* **71**, 021909 (2005).
- [7] P. A. Wiggins and P. C. Nelson, *Phys. Rev. E* **73**, 031906 (2006).
- [8] P. A. Wiggins, T. V. D. Heijden, F. Moreno-Herrero, A. Spakowitz, R. Phillips, J. Widom, C. Dekker, and P. C. Nelson, *Nature Nanotechnology* **1**, 137 (2006).
- [9] A. K. Mazur, *Biophys. J.* **91**, 4507 (2006).
- [10] A. K. Mazur, *J. Am. Chem. Soc.* **120**, 10928 (1998).
- [11] L. D. Landau and E. M. Lifshitz, *Statistical Physics, Part I* (Nauka, Moscow, 1976).
- [12] A. K. Mazur, *J. Am. Chem. Soc.* **122**, 12778 (2000).
- [13] A. K. Mazur and D. E. Kamashev, *Phys. Rev. E* **66**, 011917 (2002).
- [14] D. E. Kamashev and A. K. Mazur, *Biochemistry* **43**, 8160 (2004).
- [15] D. M. Crothers and Z. Shakked, in *Oxford Handbook of Nucleic Acid Structure*, edited by S. Neidle (Oxford University, New York, 1999), p. 455.
- [16] F. Lankas, R. Lavery, and J. H. Maddocks, *Structure* **14**, 1527 (2006).
- [17] J. Z. Ruscio and A. Onufriev, *Biophys. J.* **91**, 4121 (2006).
- [18] T. E. Cheatham, III and P. A. Kollman, *Annu. Rev. Phys. Chem.* **51**, 435 (2000).
- [19] R. E. Dickerson, *Oxford Handbook of Nucleic Acid Structure* (Oxford University, New York, 1999), p. 145.
- [20] A. K. Mazur, *J. Mol. Biol.* **290**, 373 (1999).